NASA Technical Memorandum 4281

Mass Flux Similarity for Slotted Transonic-Wind-Tunnel Walls

Joel L. Everhart
Suresh H. Goradia

AUGUST 1991

NASA

NASA Technical Memorandum 4281

Mass Flux Similarity for Slotted Transonic-Wind-Tunnel Walls

Joel L. Everhart
Langley Research Center
Hampton, Virginia

Suresh H. Goradia
ViGYAN, Inc.
Hampton, Virginia

National Aeronautics and
Space Administration

Office of Management

Scientific and Technical
Information Program

1991

Symbols

d	slot width, cm
f, g	similarity functions, see equations (2), (4), and (6)
M	Mach number
p_t	total pressure, N/m^2
U	longitudinal (axial) velocity component, m/sec
V	transverse (cross-flow) velocity component, m/sec
x	longitudinal distance (tunnel station) along tunnel, cm
y	distance normal to tunnel wall, cm
z	distance normal to X, Y plane, cm
η	similarity variable, see equation (1)
θ	flow angle measured from tunnel centerline, deg
ξ	similarity variable, see equations (3) and (5)
ρ	density, gm/cm^3

Subscripts:

s	slot
u	associated with the U velocity component
v	associated with the V velocity component
vc	vena contracta
1/2	plenum location where transverse mass flux is one half vena contracta value
1	region 1, see equation (3)
2	region 2, see equation (5)
∞	free stream

Abbreviations:

DFA	diffuser flow apparatus of National Transonic Facility
LE, TE	leading edge and trailing edge of airfoil
TE	tunnel empty
6×19	Langley 6- by 19-Inch Transonic Tunnel

Abstract

Flow-field measurements obtained in the vertical plane at several stations along the centerline of slots in two different longitudinally slotted wind-tunnel walls are discussed. The longitudinal and transverse components of the data are then transformed by the concept of flow similarity to demonstrate the applicability of the technique to the development of the viscous shear flow along and through a slotted wall of an airfoil tunnel. Results are presented that show the performance of the similarity transformations with variations in tunnel station, Mach number, and airfoil-induced curvature of the tunnel free stream.

Introduction

Accurately simulating flight conditions about an aerodynamic configuration in a wind tunnel by either experimental or computational means is a challenging problem. This is particularly true for transonic wind tunnels where tunnel-wall-induced disturbances to the flow may be extremely large at the model position, that is, where the simulation is most important. Slots or perforations are usually installed in the walls to relieve the tunnel blockage due to nonlinear transonic effects (such as shock waves and choking) and reduce the interference at the model position. The determination of appropriate corrections to the flow conditions for tunnels with these types of walls has been an area of concentrated research for the past 4 decades (for example, see Davis and Moore 1953, Garner et al. 1966, Berndt and Sörensén 1976, Newman and Barnwell 1984, and Everhart 1988). The typical correction procedure involves a theoretical simulation that spanwise averages the flow inside the tunnel over the solid and open portions of the wall. The result is a mathematical expression (or boundary condition) which relates the pressure drop across the wall to some average of the local flow properties (flow angle, streamline curvature, etc.) inside the tunnel. Unknown coefficients in the boundary condition are functions of the wall geometry and the viscous nature of the wall flow field. An understanding of the viscous behavior of the flow at and through the wind-tunnel wall is therefore a necessity for the accurate modeling of the wall boundary condition and the proper simulation of the flow about the wind-tunnel model.

Only a small number of experimental studies of the viscous, slotted-wall flow field have been reported in the literature. Berndt and Sörensén (1976) examined the effect of wall boundary-layer thickness on the slot flow. Their measurements included longitudinal surveys of the total pressure along the slot and at different depths through the slot, and longitudinal measurements of the slot flow angles on the plenum side of the wall. The influence of airfoil-induced streamline curvature on the slot flow was examined only for the condition of outflow to the surrounding plenum chamber. Wu, Collins, and Bhat (1983) examined the three-dimensional structure of the flow inside the tunnel over a baffled slot. The baffles were used to direct the flow into the plenum. Spanwise surveys were made at four longitudinal stations over a slot with a five-tube flow-angle probe. Mass flow through the slot was increased by decreasing the plenum pressure; streamline curvature of the tunnel flow was not included in the study. This study was later extended by Bhat (1988) to include measurements of a baffled slot arrangement with segmented plenum chambers. Mass flux through the wall was varied by changing the pressure in the different plenums via suction or blowing. The influence on the wall flow field was then determined. Detailed distributions of the flow characteristics along and through a slot on its centerplane were obtained during a study conducted in the diffuser flow apparatus of the National Transonic Facility with a three-tube flow-angle probe (Everhart, Igoe, and Flechner 1991). The probe was driven from a position in the tunnel where the influence of the slot was negligible through the slot to a similar "far-field" position in the plenum chamber. Limited measurements were also made with a three-tube flow-angle probe in the Langley 6- by 19-Inch Transonic Tunnel on and through a centerline slot with the tunnel empty and with an airfoil installed (Everhart 1988).

Even though the data are limited, some sense of rationality and cohesiveness can be made of those which are available. Analysis of these data indicates that similarity of the fluid flow exists along the centerplane of a slot of a longitudinally slotted wind-tunnel wall. Application of similarity methods could greatly simplify the viscous modeling of slotted-wall flows. Slotted-wall wind tunnels could be better designed to reduce the wall-induced interference on the flow over the model and thereby lead to more accurate tunnel simulations of flight conditions. Computationally, much simpler mathematical models of

the wall flow which include viscosity would result, thereby improving numerical simulations of wind-tunnel flow and its associated boundary conditions.

In this paper, slotted-wall flow-field data acquired in two airfoil wind tunnels with different slotted-wall configurations are discussed (Everhart 1988 and Everhart et al. 1991). Similarity relationships for the flow along and through a longitudinally slotted wind-tunnel wall are then given. Results that demonstrate the influence of longitudinal location, curvature of the free stream, and compressibility are presented.

DFA Experiment

A study of the flow development near a longitudinally slotted wind-tunnel wall was conducted in the diffuser flow apparatus (DFA) of the National Transonic Facility (NTF) (Everhart et al. 1991). This facility is a small-scale version of the contraction, test section, and diffuser region of the National Transonic Facility (Gentry et al. 1981). The tunnel test section, shown schematically in figure 1(a), is 46.38 cm square with slotted upper and lower walls and solid sidewalls. For this study, a basic slot geometry which is different from the standard DFA configuration was selected. Each slotted wall has six rectangular slots, each with a constant width d of 0.635 cm (totaling 8.2 percent open) and a depth of 0.61 cm. The slots originate at tunnel station 0 and terminate in the reentry region at tunnel station $\approx$114. The entry edge of the slot is a rectangular lip rather than the gradual, tapered opening that is common for most slotted-wall test sections. Figures 1(b) and 1(c) show the slot coordinate system and cross-sectional shape, respectively.

Flow angles were measured with a three-tube flow-angle probe. The probe had a width of 0.051 cm compared with the 0.635-cm width of the slot to minimize interference with the slot sidewalls. Measurements were made on the slot centerplane on one of the center slots. The probe was traversed normal to the wall at fixed longitudinal stations and also along the slot at a fixed distance normal to the slot. Test results were obtained at free-stream Mach numbers of 0.6, 0.725, and 0.85 over a range of nominal Reynolds number per meter from 10.4×10^6 to 12.5×10^6. In addition, data were acquired with various amounts of plenum suction, although only those data with zero plenum suction are presented.

The test model was an NACA 0012-64 airfoil with a 13.72-cm chord. For this airfoil, the maximum thickness occurs at 40-percent chord which corresponds to tunnel station 62.89. The tunnel semiheight-to-chord ratio is 1.67, which is typical for two-dimensional airfoil testing. All data were acquired with the airfoil installed at an angle of attack of 0° (zero lift for this model).

The transverse development of the tunnel-empty slot flow at four longitudinal stations is shown in figure 2 for a free-stream Mach number of 0.6. For each station, the local flow angle, Mach number, and total pressure ratio are plotted against the vertical distance measured from the wall y/d, where the slot width is used for normalization. In this coordinate system, y/d of 0 is at the slot entrance and positive displacements are into the tunnel. Positive flow angle is measured toward the plenum. (See fig. 1(a).) In figure 2(a), the flow angle in the tunnel is seen to be very small, and it increases rapidly (in approximately 2 slot widths) to about 7° of outflow at the slot entrance. The flow angle increases almost linearly from 3° at $y/d \approx 0.4$ to its maximum value of approximately 11° at $y/d \approx -0.4$. At this point, the flow passes through the vena contracta or the minimum "fluid" (as opposed to "geometric") slot width. The transverse mass flux per unit area ρV will also maximize near $y/d \approx -0.4$ (Everhart 1988). The local Mach number and local total pressure ratio given in figures 2(b) and 2(c) show an expected decrease due to shearing of the flow in the vicinity of the wall. Measured values of the total pressure in the slot are about 91 percent of their free-stream values.

Another interesting point to note in figure 2 is the development and stabilization of the shear layer. An overexpansion of the flow into the plenum can be seen in the most upstream set of flow-angle measurements (fig. 2(a)) at tunnel station 20.32. This overexpansion occurs as the flow responds to the sudden opening of the slot and the sudden appearance of a pressure drop across the wall. Full stabilization occurs somewhere between stations 40.64 and 60.96. Flow stabilization is also apparent in the Mach number (fig. 2(b)) and total pressure (fig. 2(c)) plots (particularly in the latter).

The effect of increasing the tunnel-empty, free-stream Mach number from 0.6 to 0.85 is shown in figure 3 for tunnel station 60.96. The flow angles (fig. 3(a)) are essentially the same for these two Mach numbers. Variations in the Mach number profiles (fig. 3(b)) are as expected and give an indication of the penetration of the tunnel flow into the plenum. The viscous slot flow is contained in a region of approximately 4 slot widths near the wall (fig. 3(c)). The increased shearing of the flow near the wall and in the slot at the higher Mach number decreases the total pressure ratio from 0.91 to 0.82.

The data at tunnel station 60.96 with and without the airfoil installed are shown in figure 4 for a free-stream Mach number of 0.6. At this station all slot flow variables with the airfoil installed are smaller than the corresponding tunnel-empty values. When the airfoil is installed, its presence has the global effect of increasing the pressure drop across the wall which subsequently increases the angle of the flow through the slots far from the model. In other words, the flow begins adjusting to the presence of the model far upstream. Near the model, large gradients are created in the flow by the requirement that the flow go around the model, through the slot, and reenter the tunnel downstream of the position of maximum model thickness. These gradients dominate the slot flow which (for the case under consideration) has a slot flow angle of approximately 0° at the maximum model thickness. The measurements presented are just upstream of the maximum airfoil thickness and thus are near the station where the flow angles of the streamlines around the airfoil are reversing in sign. This turning of the flow brings the lower momentum air from the plenum farther into the slot and decreases the local Mach number (fig. 4(b)) and local total pressure (fig. 4(c)). Further explanation of this phenomena may be found in Everhart (1988). It is also significant to note that the vena contracta occurs at approximately the same location as that for the tunnel-empty case.

An interesting phenomenon occurs in the flow-angle data (fig. 4(a)) between $1 \leq y/d \leq 2$ with the airfoil installed. In this region, the flow begins changing direction and approaches zero before it again accelerates into the slot. Unfortunately, this was the only tunnel station where measurements were made with the airfoil installed, and the exact reason for this behavior is unknown. One possible explanation is found in data presented by Wu et al. (1983) and Bhat (1988). In these tunnel-empty experiments, measurements of the three velocity components were made with a five-tube flow-angle probe over a single longitudinal slot which contained zig-zag-shaped baffles. These measurements were then projected onto the plane normal to the tunnel free stream. For a case with no plenum suction, these data revealed the existence of a vortexlike secondary motion on each side of the slot. When suction was applied, the vortex disappeared, and the flow was strongly directed toward the slot. Although these experiments did not probe a true longitudinally slotted-wall flow field (because of the presence of the baffles), the general character of the data for outflow to the plenum should be representative of that over a slotted wall. By analogy with these results, for the tunnel-empty DFA data, the pressure drop across the wall is large enough for the normal velocity to increase monotonically through the slot to the vena contracta. However, the presence of the airfoil introduces an effective suction in the test section; thus the local pressure drop across the wall is reduced. This could allow the formation of a vortex pair which would give the flow angle a behavior like that shown in figure 4(a).

6- by 19-Inch Transonic Tunnel Experiment

An experiment (Everhart 1988) which included measurements of the flow properties in the vicinity of the slotted wind-tunnel wall was conducted in the Langley 6- by 19-Inch Transonic Tunnel (6×19) (Ladson 1973). This two-dimensional wind tunnel is 15.24 cm wide by 48.26 cm high and has solid sidewalls and slotted upper and lower walls. The tunnel is an atmospheric blowdown facility with a range of Mach number from 0.1 to 1.2 and a range of Reynolds number per meter from 16.0×10^6 to 26.0×10^6. Schematically, this facility is similar to that shown in figure 1(a).

The airfoil model used during the experiment was a symmetrical NACA 0012 airfoil with a 15.24-cm chord, which was mounted on the tunnel centerline. For the measurements presented, the top and bottom walls each contained a single, rectangular-cross-section centerline slot which was 15 percent of the wall area. Each slot opened linearly over a length of 6 in. from fully closed to a width of 2.286 cm and then extended downstream at constant width for 91.44 cm. The slot depth was 0.318 cm. During the experiment, measurements were made at free-stream Mach numbers from 0.1 to 0.80.

The flow angles were measured with a three-tube flow-angle probe on the slot centerplane at a tunnel station 1/2 chord upstream of the airfoil leading-edge station. Measurements were made with the tunnel empty and with the airfoil installed at zero lift. Typical flow-angle results presented in figure 5 are plotted against vertical displacement from the wall normalized by the slot width y/d for a free-stream Mach number of 0.7. The flow at this upstream location with the airfoil installed is beginning its expansion around the model which results in an increase in the magnitude of the flow angle at the vena contracta. Mach number and total pressure results similar to those shown in figure 3 for the DFA experiment were also obtained and are available for analysis but are not presented.

Definition of Similarity Relations

Analysis of the flow-field data from these two experiments indicated that by using an appropriate set of similarity transformations, the data on the slot centerplane could be collapsed to two curves: one for the longitudinal (or streamwise) component of the flow and one for the transverse (or cross-flow) component. Prior to presenting the similarity relations and results, however, several parameters must be defined.

Local values of the longitudinal and transverse mass flux (ρU and ρV, respectively) in the vicinity of the wall were calculated from the flow angle, Mach number, and total pressure measurements for both data sets. The location y_{vc} where the maximum of the cross-flow component occurs (i.e., the vena contracta) was then determined from the computed transverse mass flux distributions. Next, longitudinal mass flux values at this location were obtained by interpolation. The position in the plenum where the transverse mass flux measured one half that at the vena contracta $y_{1/2}$ was also determined.

Free-stream mass flux values were determined at the locations $y_{u,\infty}$ and $y_{v,\infty}$ where the subscripts u and v represent longitudinal and transverse directions, respectively. The subscript ∞ denotes an actual free-stream position interpolated from the data in the DFA experiment; however, for the 6×19 experiment the subscript ∞ indicates the value of the data measured farthest from the wall toward the free stream of the tunnel. This definition was used for the 6×19 data because of the uncertainty in knowing whether the probe was traversed far enough away from the slot into the tunnel for an appropriate measurement of the local free-stream conditions. (See fig. 5.) Longitudinal free-stream components were defined according to

$$\frac{\rho U}{(\rho U)_\infty} = 0.995$$

and the transverse component according to

$$\frac{\rho V - (\rho V)_{vc}}{(\rho V)_\infty - (\rho V)_{vc}} = 0.995$$

With these definitions, a discussion about the similarity transformations is appropriate. An examination of the flow-field measurements indicated that a single relationship characterizing the longitudinal mass flux component could be developed for the entire region extending from the tunnel free stream into the undisturbed plenum. The definitions of the longitudinal similarity variables for this region are

$$\eta = \frac{y - y_{vc}}{y_{u,\infty} - y_{vc}} \tag{1}$$

and

$$f(\eta) = \frac{\rho U - (\rho U)_{vc}}{(\rho U)_\infty - (\rho U)_{vc}} \tag{2}$$

A similar examination of the transverse flow-field data indicated the existence of at least two regions in the cross flow. The first of these is an acceleration into the slot up to the vena contracta, and the second is a deceleration from the vena contracta into the plenum. The similarity transformations describing the first region are

$$\xi_1 = \frac{y - y_{vc}}{y_{v,\infty} - y_{vc}} \tag{3}$$

and

$$g(\xi_1) = \frac{\rho V - (\rho V)_{vc}}{(\rho V)_\infty - (\rho V)_{vc}} \tag{4}$$

Similarity transformations for the second region are given by

$$\xi_2 = \frac{y_{vc} - y}{y_{1/2} - y_{vc}} \tag{5}$$

and

$$g(\xi_2) = \frac{\rho V - (\rho V)_{vc}}{(\rho V)_{1/2} - (\rho V)_{vc}} \tag{6}$$

Performance of Similarity Transformations

The tunnel-empty DFA data have been used to demonstrate the validity of the similarity transformations and their dependence on axial location. These results are presented in figure 6 with the data from different tunnel wall axial stations for a free-stream Mach number of 0.6. Excellent correlations of the similarity transformations, $f(\eta)$ and $g(\xi)$, are shown to exist with transformed normal displacements, η and ξ, respectively, over the entire extent of the slotted wall. Scatter in $g(\xi)$ near $\xi = 0.5$ is a result of the shear layer stabilization after the initial slot opening effects. (See fig. 2(a).) The goodness of the correlations indicates that for these conditions, the boundary layer is fully developed over the wall (not an unexpected result) and that away from the initial slot opening effects, the slot shear layer is well-defined and behaves such that its growth characteristics are known. For instance, the location of the vena contracta consistently occurred at approximately

0.3–0.5 slot widths from the slot-lip-entry edge into the plenum (fig. 2(a)). This distance is probably set by the sharp edge of the slot geometry which fixes the separation point of the wall cross flow (Everhart 1988). Likewise, the $y_{1/2}$ point seems to be similarly "fixed," but a definite statement of this cannot be made because of instrument resolution problems which occur when using flow-angle probes at small values of dynamic pressure (like those occurring here, which are deep in the plenum).

Mach number and wall geometry effects on the tunnel-empty results are examined in figure 7, where data are given from both the DFA and the 6×19. These data were acquired over and through two different slotted-wall geometry configurations, one with an 8.2-percent-open wall (DFA) and one with a 15-percent-open wall (6×19). Implicit in these results are facility-related details such as different tunnel-wall boundary layers and different unit Reynolds numbers. The transformed mass flux values, again, correlate well with the transformed coordinates almost everywhere. Exceptions are for $f(\eta)$ near $\eta = -1$, which is in the plenum at the edge of the shear layer where small values of dynamic pressure make the velocities difficult to determine, and for $g(\xi)$ in the region $0.25 \leq \xi \leq 0.75$ for the cross-flow variable. In this latter region, the 6×19 data differ slightly from the DFA data. The mismatch appears attributable to not having a good definition of position $y_{v,\infty}$, where the transverse free-stream conditions are reached for the 6×19 (fig. 5). Mach number effects are insignificant for both the longitudinal and transverse variables. Variations in wall geometry (for like cross-sectional shapes) and facility effects are insignificant for the longitudinal variable; however, the transverse variable does exhibit some differences between the DFA and the 6×19 results. These differences will, in all likelihood, disappear with a more precise definition of the transverse scaling ξ which includes the free-stream position $y_{v,\infty}$.

The influence of airfoil-induced curvature of the free stream and additional effects of compressibility on the similarity transformations are shown in figure 8. Longitudinal similarity results for both facilities are presented in figure 8(a). The 6×19 results were taken at a station 1/2 chord upstream of the airfoil leading edge where the curvature of the flow in the slot, $d\theta_s/dx$, is nearly zero, and the DFA results were obtained near the point of maximum airfoil thickness where the curvature of the slot flow is near its maximum value (Everhart 1988). A tunnel-empty result is also shown. Very good tunnel-to-tunnel correlation exists between these two data sets.

The effect of stream curvature on the transverse variables at $M_\infty = 0.6$ is shown for the DFA with and without the model in figure 8(b). (Similar results were obtained for $M_\infty = 0.725$.) The similarity transformations do not collapse the data as well in this case as they did for the other cases considered and are plotted as lines to highlight the differences. Significant differences occur deep in the plenum ($\xi = \xi_2 < -1.5$) because the instrumentation could not resolve small values of dynamic pressure. Also, correlations of the similarity transformations in the vicinity of $\xi = \xi_1 = 0.5$ are not as good as would be desired; however, these deviations are not unexpected because of the previously cited characteristics of the flow-angle measurements presented and discussed in figure 4(a). The sparseness of the experimental data base permits only speculation that there exists another region, $0.5 \leq \xi \leq 1$, where similar flows and similarity transformations may be shown to exist. The scaling in this region may depend on some value of the local shear stress or some value of the wall boundary-layer thickness.

Formulation of the similarity relations in the manner presented, although not firmly established for the cross-flow component with free-stream curvature, opens the way for a simplified solution of the viscous flow which exists on slotted wind-tunnel walls. Further experimental research should be conducted using nonintrusive measurement techniques to tie the present results to those existing over the solid portions of the wall and to further examine the behavior of the flow with curvature of the free stream. The influence of the cross-sectional geometry of the slot should be evaluated as should the thickness of the wall boundary layer over the slot. Additional variations in the tunnel test conditions, such as airfoil lift, plenum suction (large tunnel-wall outflow), and plenum pressurization (tunnel-wall inflow), should also be considered in future investigations.

Concluding Remarks

The present analyses have shown that the shear layer in the wall region of a longitudinally slotted wind tunnel can be described with the concept of flow similarity. Mass flux similarity relations have been developed and applied to the tunnel-wall flowfield data acquired in two wind tunnels with different slotted-wall geometries. The results show excellent correlation of the longitudinal and transverse flow components in the absence of free-stream curvature and in the longitudinal component with curvature. Cross-flow correlations in the presence of airfoil-induced curvature of the free stream, although generally good, indicate the possible existence of an

additional region where similarity relationships can be defined, but until additional data are acquired, the existence of this region is only speculative. The results indicate the choice of similarity parameters to be insensitive to the effects of compressibility from low subsonic through transonic Mach numbers. Comparisons between the data acquired in the two different wind-tunnel facilities where different wall geometries and wall boundary layers existed showed excellent longitudinal correlation; however, some differences existed in the transverse direction. These differences are believed to result from not having traversed the flow-angle probe far enough into the tunnel free stream to properly delineate the wall boundary flow field from the mainstream flow in the tunnel. With the proper definition of this boundary, the transverse scaling should appropriately correlate the two sets of data, and any differences should be removed.

NASA Langley Research Center
Hampton, VA 23665-5225
May 10, 1991

References

Berndt, Sune B.; and Sörensén, Hans: Flow Properties of Slotted Walls for Transonic Test Sections. *Windtunnel Design and Testing Techniques,* AGARD-CP-174, Mar. 1976, pp. 17-1–17-10.

Bhat, Maharaj Krishen: On Transonic Flow Over Segmented Slotted Wind Tunnel Wall With Mass Transfer. Ph.D. Thesis, Univ. of Tennessee, 1988.

Davis, Don D., Jr.; and Moore, Dewey: *Analytical Study of Blockage- and Lift-Interference Corrections for Slotted Tunnels Obtained by the Substitution of an Equivalent Homogeneous Boundary for the Discrete Slots.* NACA RM L53E07b, 1953.

Everhart, Joel Lee: Theoretical and Experimental Studies of the Transonic Flow Field and Associated Boundary Conditions Near a Longitudinally-Slotted Wind-Tunnel Wall. D.Sci. Diss., George Washington Univ., Feb. 14, 1988. (Available as NASA TM-103381.)

Everhart, Joel L.; Igoe, William B.; and Flechner, Stuart G.: *Slotted-Wall Flow Field Measurements in a Transonic Wind Tunnel.* NASA TM-4280, 1991.

Garner, H. C.; Rogers, E. W. E.; Acum, W. E. A.; and Maskell, E. C.: *Subsonic Wind Tunnel Wall Corrections.* AGARD-AG-109, Oct. 1966.

Gentry, Garl L., Jr.; Igoe, William B.; and Fuller, Dennis E.: *Description of 0.186-Scale Model of High-Speed Duct of National Transonic Facility.* NASA TM-81949, 1981.

Ladson, Charles L.: *Description and Calibration of the Langley 6- by 19-Inch Transonic Tunnel.* NASA TN D-7182, 1973.

Newman, Perry A.; and Barnwell, Richard W., eds.: *Wind Tunnel Wall Interference Assessment/Correction—1983.* NASA CP-2319, 1984.

Wu, J. M.; Collins, F. G.; and Bhat, M. K.: Three-Dimensional Flow Studies on a Slotted Transonic Wind Tunnel Wall. *AIAA J.,* vol. 21, no. 7, July 1983, pp. 999–1005.

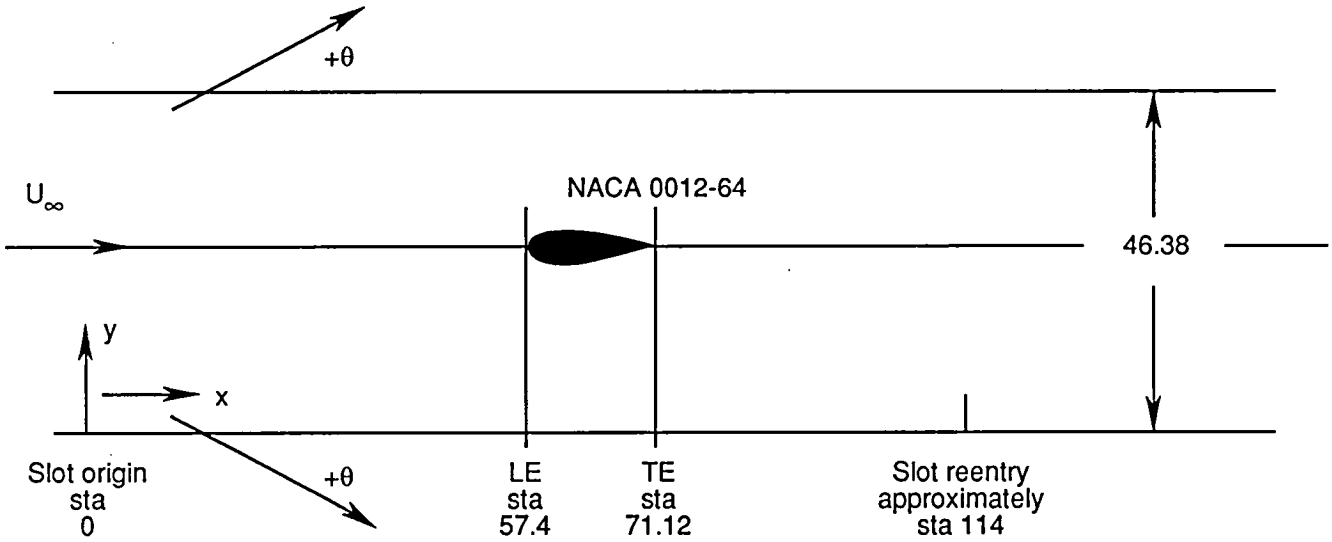

(a) Schematic of test section.

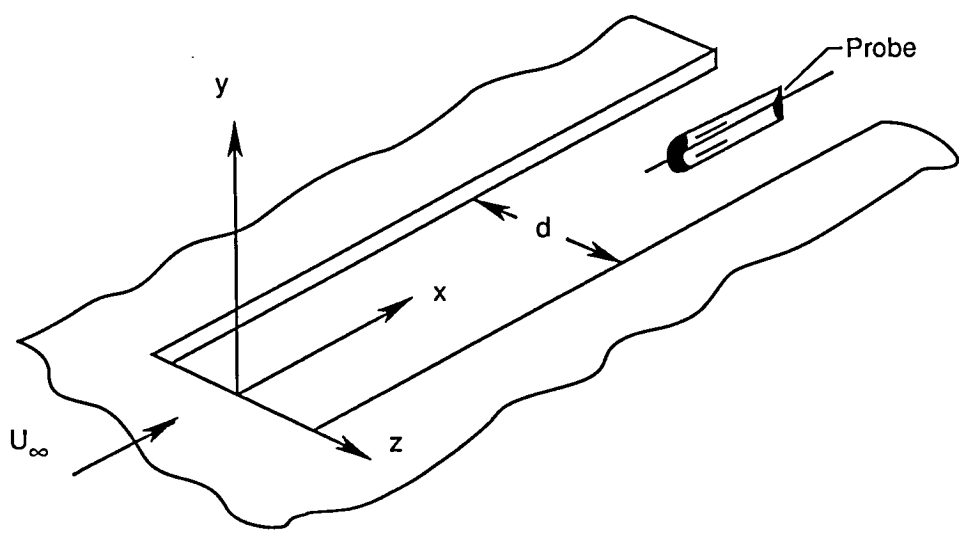

(b) Coordinate system looking inside test section.

Figure 1. Test section of DFA. Dimensions are in centimeters.

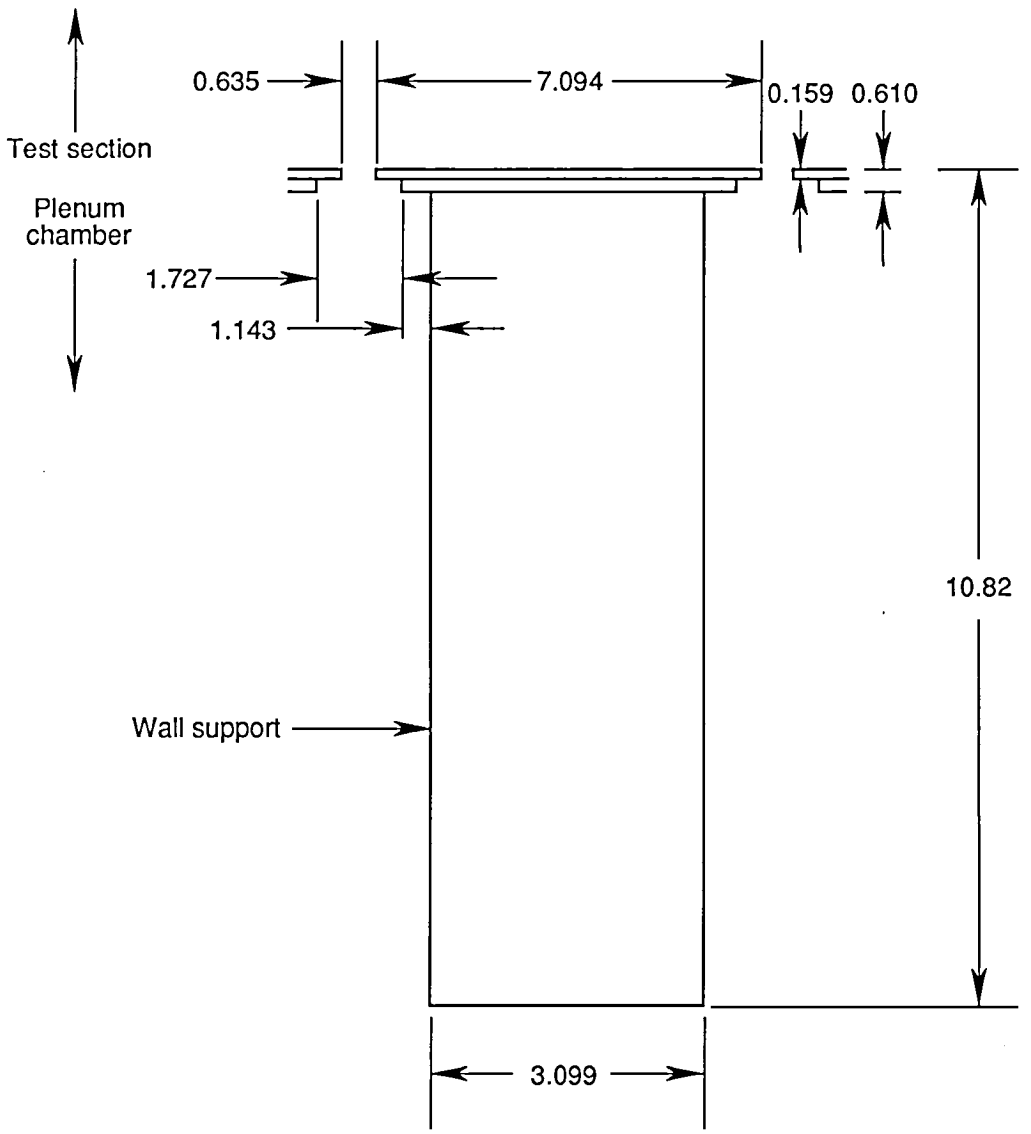

(c) Sectional view of DFA wall.

Figure 1. Concluded.

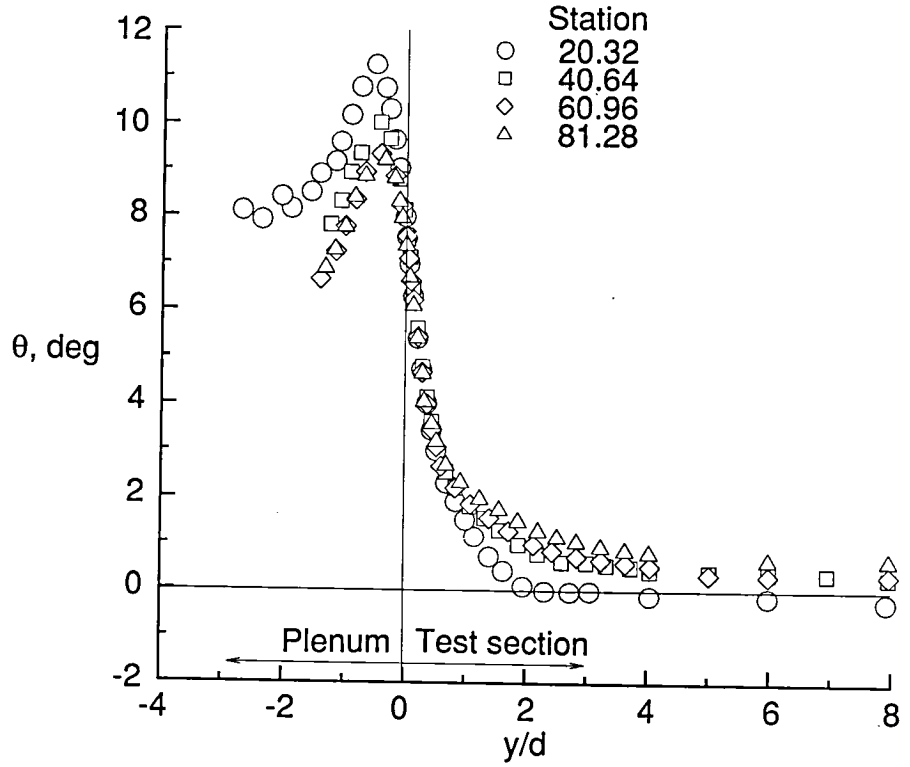

(a) Flow angle.

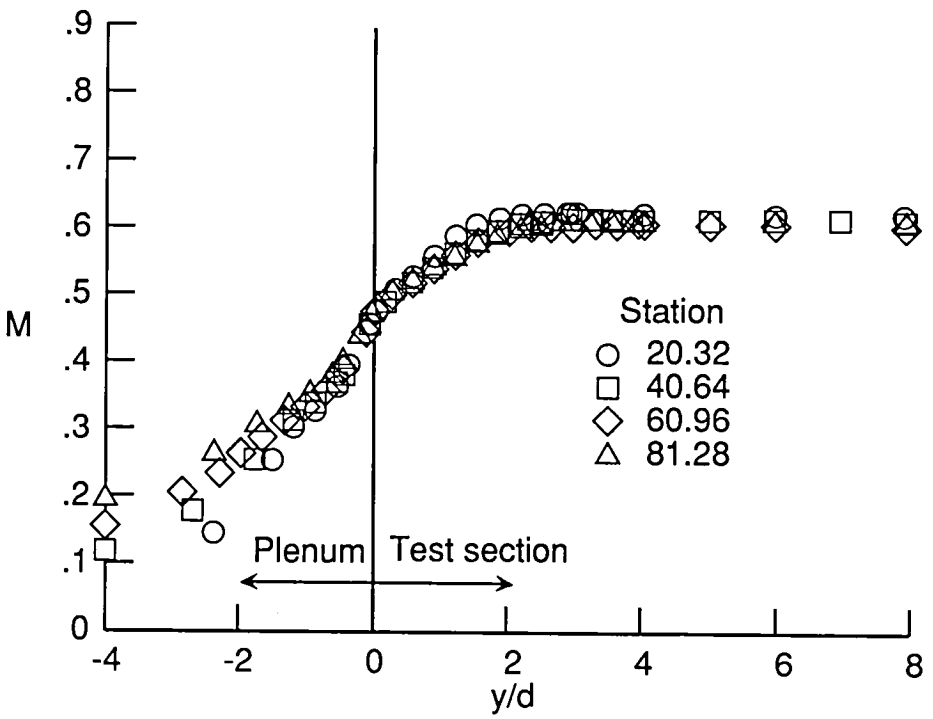

(b) Mach number.

Figure 2. Longitudinal and transverse development of tunnel-empty, local flow properties measured through slot of DFA for $M_\infty = 0.6$.

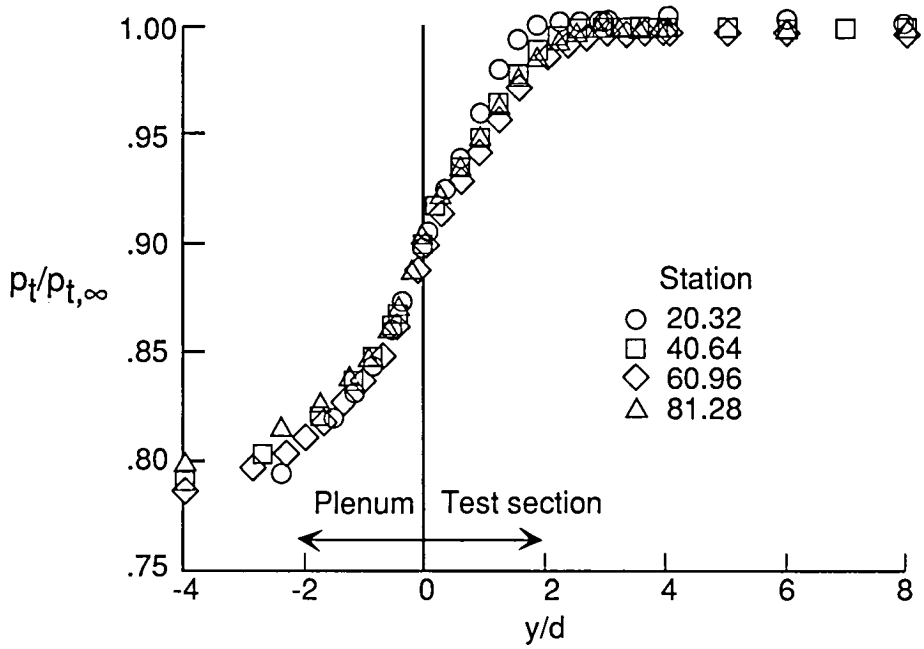

(c) Total pressure ratio.

Figure 2. Concluded.

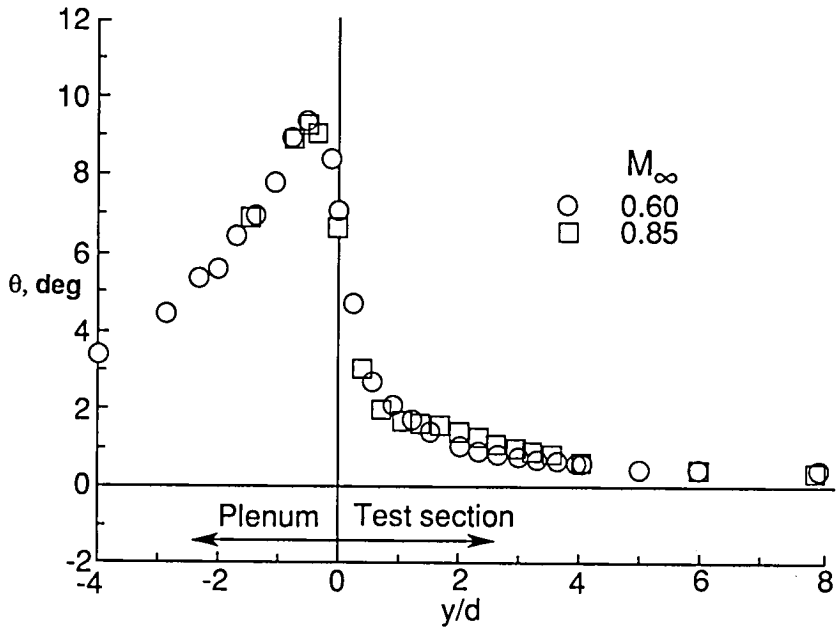

(a) Flow angle.

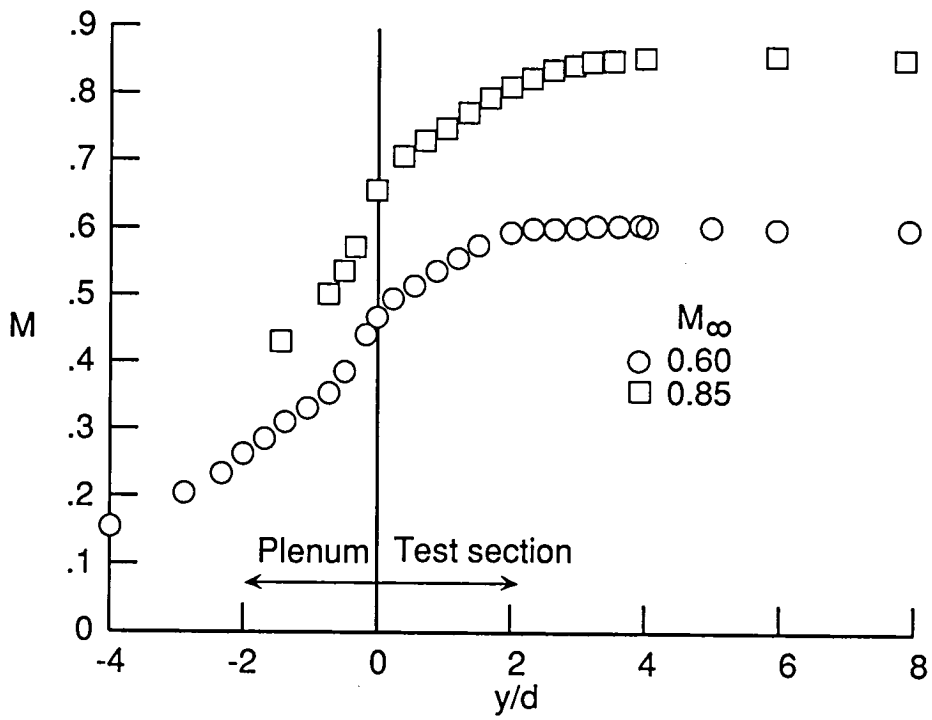

(b) Mach number.

Figure 3. Effect of tunnel-empty, free-stream Mach number on local slot flow properties measured in DFA at tunnel station 60.96 cm.

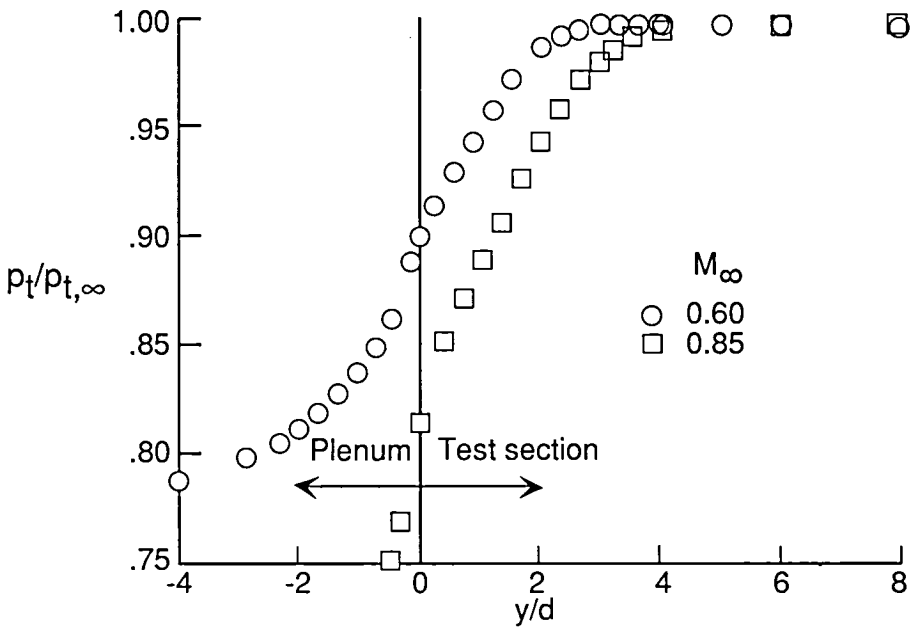

(c) Total pressure ratio.

Figure 3. Concluded.

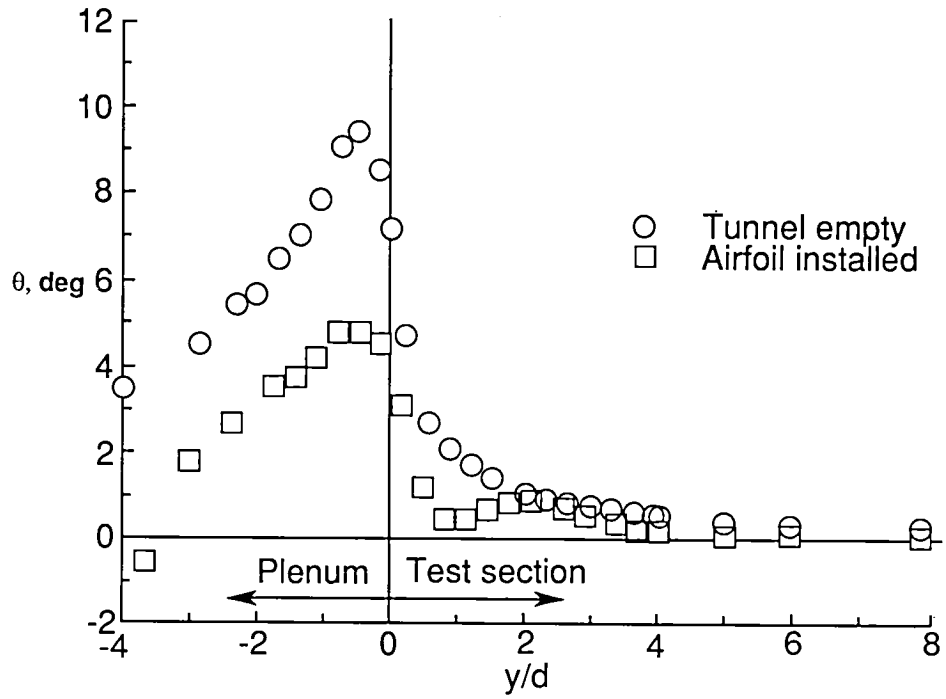

(a) Flow angle.

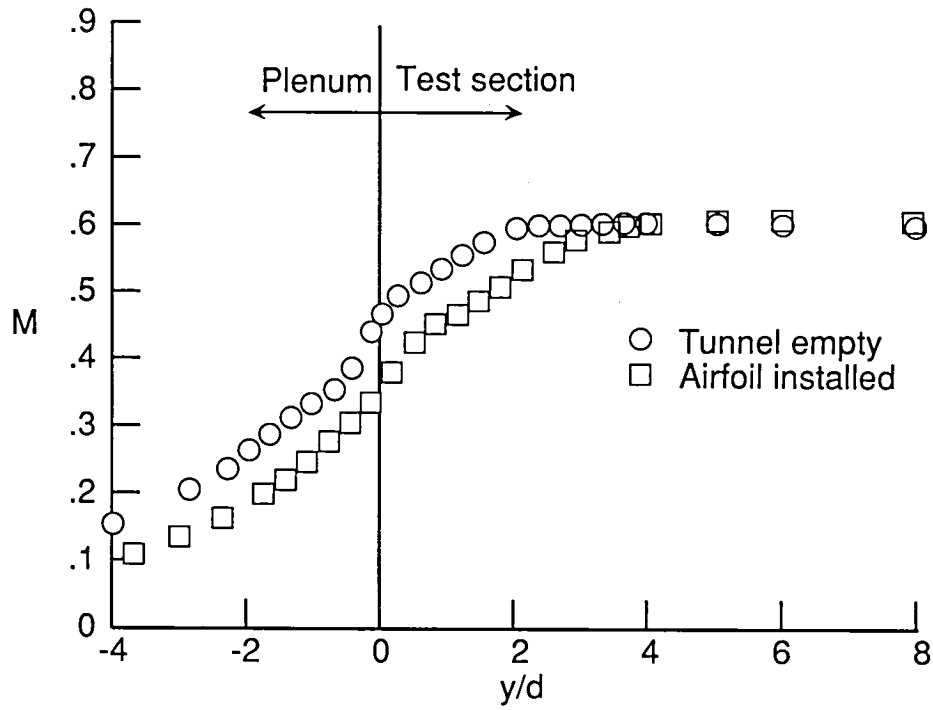

(b) Mach number.

Figure 4. Influence of airfoil-induced curvature on local slot flow properties measured in DFA at tunnel station 60.96 cm for $M_\infty = 0.6$.

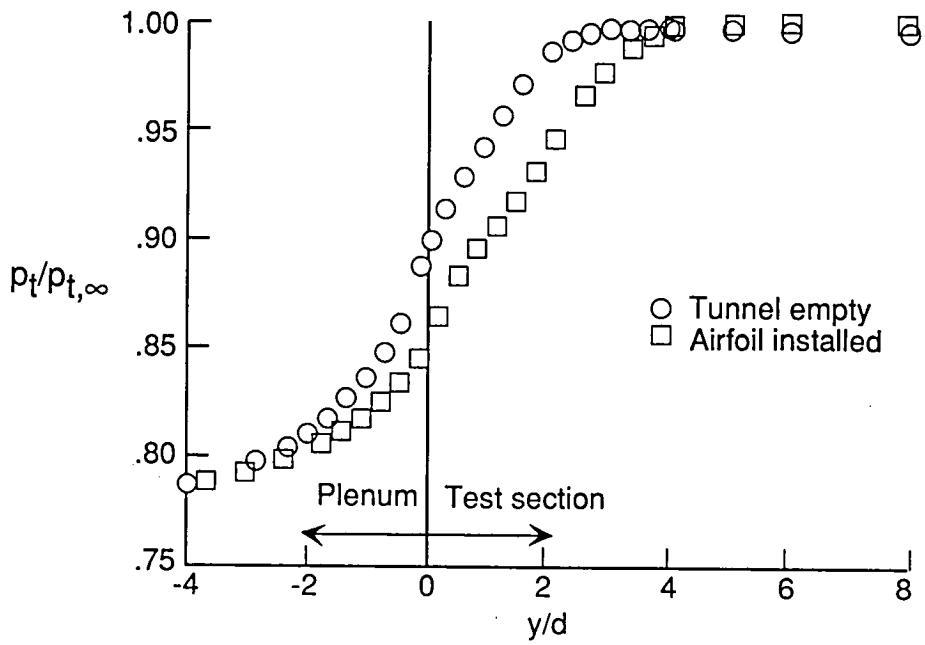

(c) Total pressure ratio.

Figure 4. Concluded.

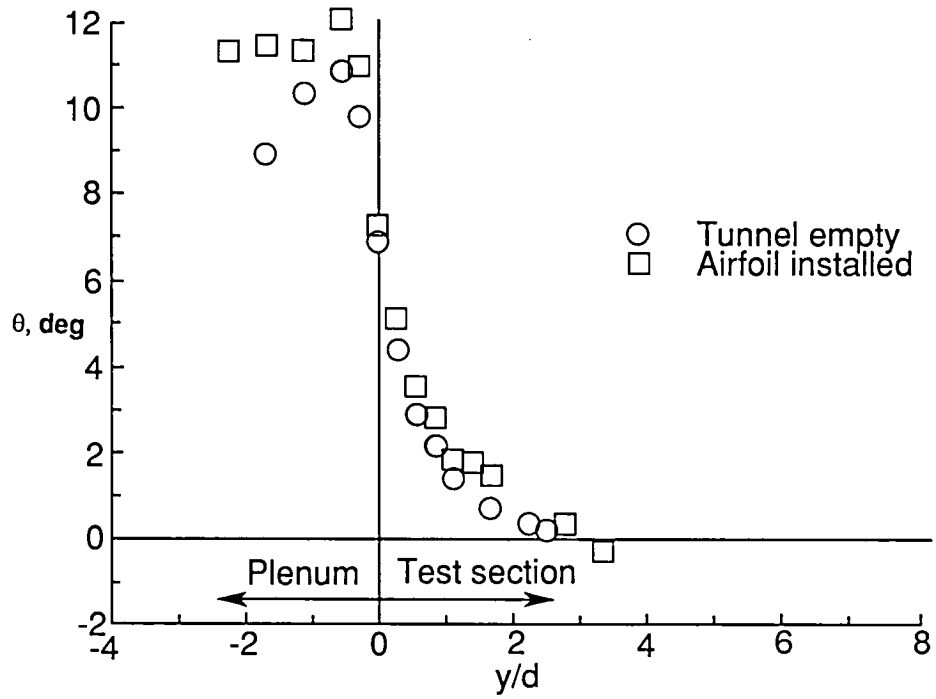

Figure 5. Slot flow angles measured in 6×19 at 1/2 chord upstream of model leading-edge station for $M_\infty = 0.7$.

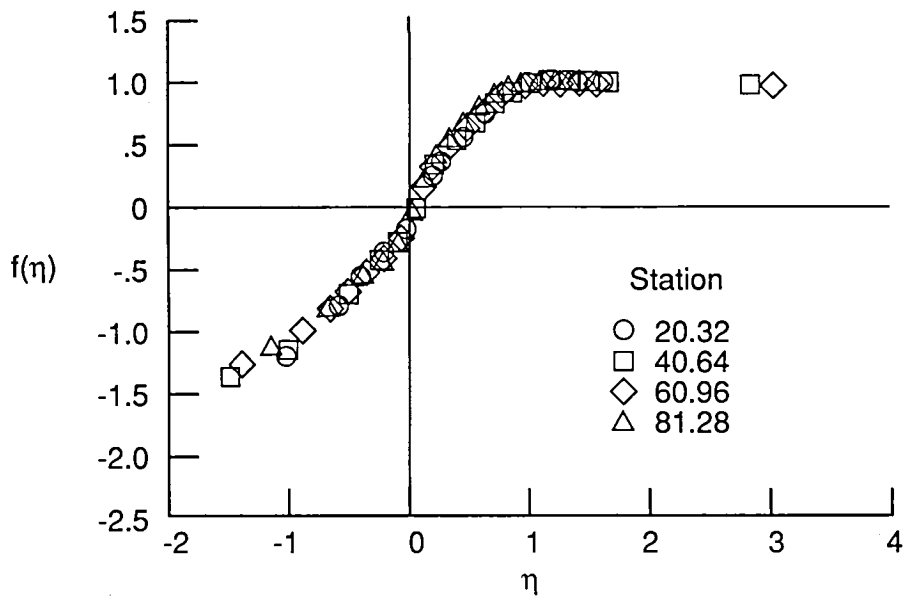

(a) Longitudinal similarity parameter.

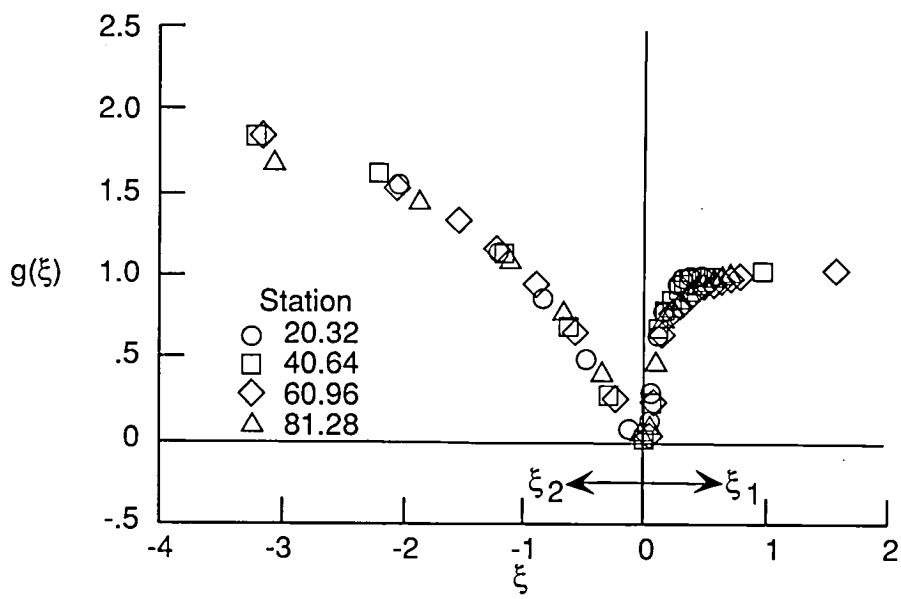

(b) Transverse similarity parameter.

Figure 6. Variation of similarity parameters with tunnel station for DFA data set for $M_\infty = 0.6$.

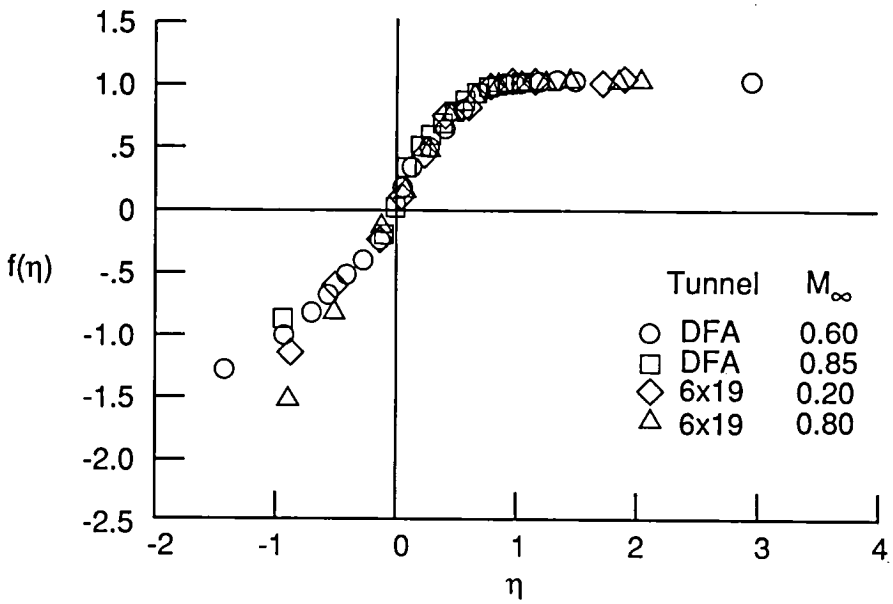

(a) Longitudinal similarity parameter.

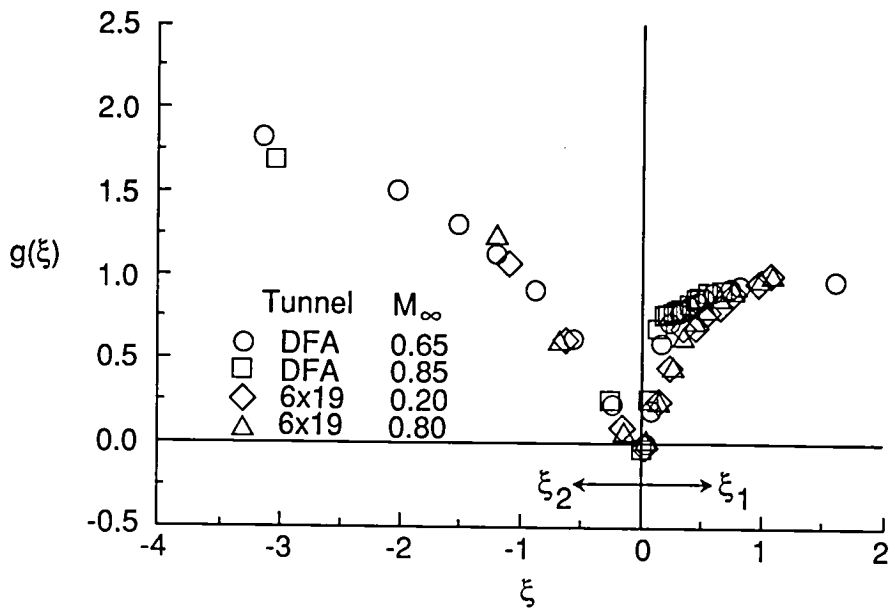

(b) Transverse similarity parameter.

Figure 7. Influence of free-stream Mach number on similarity parameters.

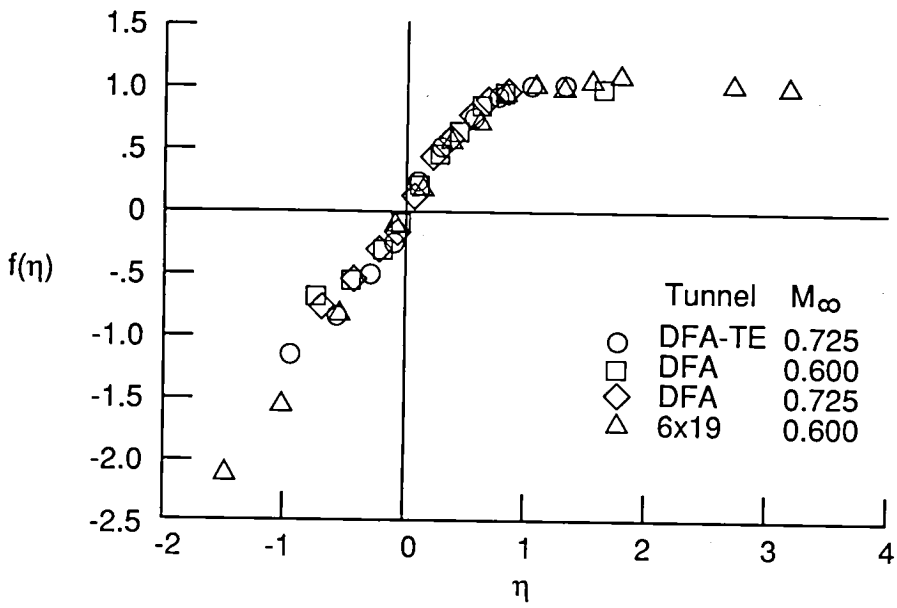

(a) Longitudinal similarity parameter.

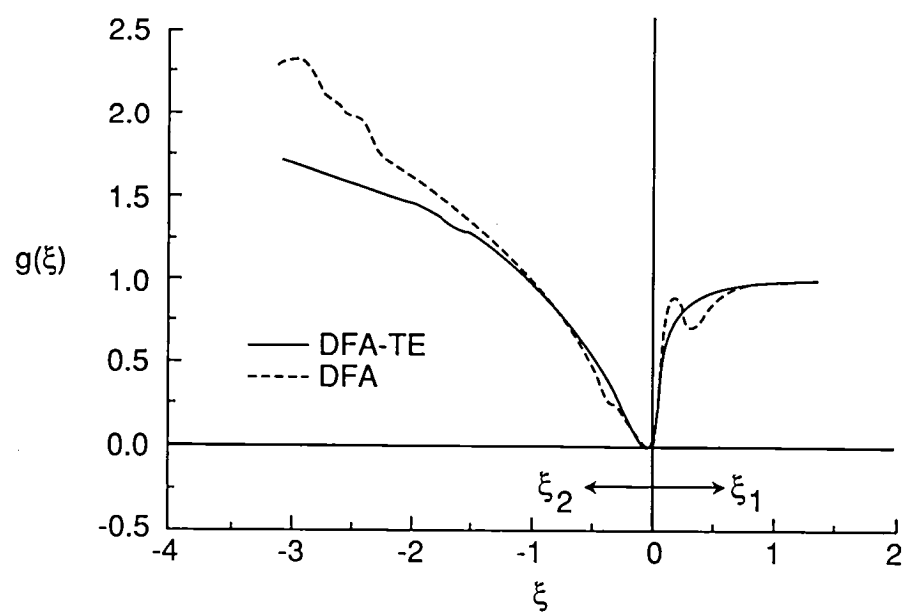

(b) Transverse similarity parameter.

Figure 8. Influence of airfoil-induced streamline curvature on similarity parameters.

NASA
National Aeronautics and Space Administration

Report Documentation Page

1. Report No.	2. Government Accession No.	3. Recipient's Catalog No.
NASA TM-4281		

4. Title and Subtitle	5. Report Date
Mass Flux Similarity for Slotted Transonic-Wind-Tunnel Walls	August 1991
	6. Performing Organization Code

7. Author(s)	8. Performing Organization Report No.
Joel L. Everhart and Suresh H. Goradia	L-16864
	10. Work Unit No.
	506-40-41-02

9. Performing Organization Name and Address	11. Contract or Grant No.
NASA Langley Research Center Hampton, VA 23665-5225	

12. Sponsoring Agency Name and Address	13. Type of Report and Period Covered
National Aeronautics and Space Administration Washington, DC 20546-0001	Technical Memorandum
	14. Sponsoring Agency Code

15. Supplementary Notes

Joel L. Everhart: Langley Research Center, Hampton, Virginia.
Suresh H. Goradia: ViGYAN, Inc., Hampton, Virginia.

16. Abstract

Flow-field measurements obtained in the vertical plane at several stations along the centerline of slots in two different longitudinally slotted wind-tunnel walls are discussed. The longitudinal and transverse components of the data are then transformed by the concept of flow similarity to demonstrate the applicability of the technique to the development of the viscous shear flow along and through a slotted wall of an airfoil tunnel. Results are presented that show the performance of the similarity transformations with variations in tunnel station, Mach number, and airfoil-induced curvature of the tunnel free stream.

17. Key Words (Suggested by Author(s))	18. Distribution Statement
Wind tunnels Transonic flow Wall interference Slotted walls Similarity	Unclassified—Unlimited Subject Category 02

19. Security Classif. (of this report)	20. Security Classif. (of this page)	21. No. of Pages	22. Price
Unclassified	Unclassified	21	A03

For sale by the National Technical Information Service, Springfield, Virginia 22161-2171